

## Equation of state of QCD at finite chemical potential from an alternative expansion scheme

---

**Paolo Parotto,<sup>a,b,\*</sup> Szabolcs Borsányi,<sup>b</sup> Zoltan Fodor,<sup>a,b,c,d</sup> Jana N. Guenther,<sup>b</sup> Ruben Kara,<sup>b</sup> Sandor D. Katz,<sup>e</sup> Attila Pásztor,<sup>e</sup> Claudia Ratti<sup>f</sup> and Kalman K. Szabó<sup>b,d</sup>**

<sup>a</sup>*Pennsylvania State University, Department of Physics, State College, PA 16801, USA*

<sup>b</sup>*University of Wuppertal, Department of Physics, Wuppertal D-42119, Germany*

<sup>c</sup>*Inst. for Theoretical Physics, ELTE Eötvös Loránd University, Pázmány P. sétány 1/A, H-1117 Budapest, Hungary*

<sup>d</sup>*Jülich Supercomputing Centre, Forschungszentrum Jülich, D-52425 Jülich, Germany*

<sup>e</sup>*Eötvös University, Budapest 1117, Hungary*

<sup>f</sup>*Department of Physics, University of Houston, Houston, TX 77204, USA*

*E-mail: [paolo.parotto@gmail.com](mailto:paolo.parotto@gmail.com)*

The equation of state of Quantum Chromodynamics (QCD) at finite density is currently known only in a limited range in the baryon chemical potential  $\mu_B$ . This is due to fundamental shortcomings of traditional methods such as Taylor expansion around  $\mu_B = 0$ . In this contribution, we present an alternative scheme [1] that displays substantially improved convergence over the Taylor expansion method. We calculate the alternative expansion coefficients in the continuum, and show our results for the thermodynamic observables up to  $\mu_B/T \leq 3.5$ .

*The 38th International Symposium on Lattice Field Theory, LATTICE2021 26th-30th July, 2021  
Zoom/Gather@Massachusetts Institute of Technology*

---

\*Speaker

## 1. Introduction

The QCD equation of state has been the subject of intense effort from the lattice community for over a decade. At vanishing baryon density, where we know the transition is a smooth crossover [2], continuum extrapolated results with physical quark masses have been available for a few years, with results from different collaborations showing excellent agreement [3–5]. At non-zero chemical potential, though, owing to the infamous complex action problem, direct simulations have not been possible. Thus, results at finite baryon density have been produced by relying on some kind of extrapolation from simulations at zero or imaginary chemical potentials. Although promising new techniques are being developed, that allow for direct simulations at finite chemical potential, these have not yet been applied to large-scale QCD simulations [6–9].

The primary means by which the extrapolation to finite chemical potential is carried out are Taylor expansion and analytical continuation from imaginary chemical potential [10–13]. In the Taylor expansion method, as the name suggests,  $\hat{\mu}_B$ -derivatives<sup>1</sup> of the partition function are calculated, from which thermodynamic quantities can then be reconstructed [14, 15]. In the case of analytical continuation from imaginary chemical potential, quantities of interest are calculated at different values of the chemical potential itself, then an extrapolation is carried out to describe the behavior at finite (real) chemical potential, often resulting in improved signal. A recent example is the study of the transition line of QCD, which is now known to great accuracy up to next-to-leading order in the baryon chemical potential, for which the two methods are in good agreement, although the analytical continuation from imaginary chemical potential shows improved uncertainty [16, 17].

Other approaches, beyond the lattice allow for the study of the QCD phase diagram. For temperatures of  $T \gtrsim 300$  MeV, perturbative methods are in quantitative agreement with lattice results (see e.g., Refs. [18, 19]). Functional methods also provide an alternative for studying the QCD phase diagram [20]. Especially in the transition region of QCD, though, lattice methods still represent the major tool of investigation.

The equation of state of QCD is of intrinsic interest in the study of the properties of strongly interacting matter. Furthermore, it plays an crucial role in the study of heavy-ion collisions, as well as in the physics of high-density objects such as neutron stars [21]. In heavy-ion collision experiments, the phase diagram of QCD can be probed by varying the collision energy. Crucially, the equation of state is a fundamental input for the hydrodynamic simulations used to study the experimental results, but its knowledge from first principles is still limited in its  $\hat{\mu}_B$  range. Significant computational efforts was placed with the goal of extending the reach of the Taylor expansion, yet even the sixth  $\hat{\mu}_B$ -derivative of the QCD pressure is currently available with modest precision [14, 15].

We illustrate in these proceedings a new scheme for extrapolating the equation of state of QCD to larger chemical potential, which we devised to be tailored to the specific problem at hand [1]. We are then able to considerably improve the convergence properties when compared to the Taylor approach, and thus reach larger values of the chemical potential. We present continuum extrapolated results for thermodynamics observables at chemical potentials as high as  $\hat{\mu}_B = 3.5$ .

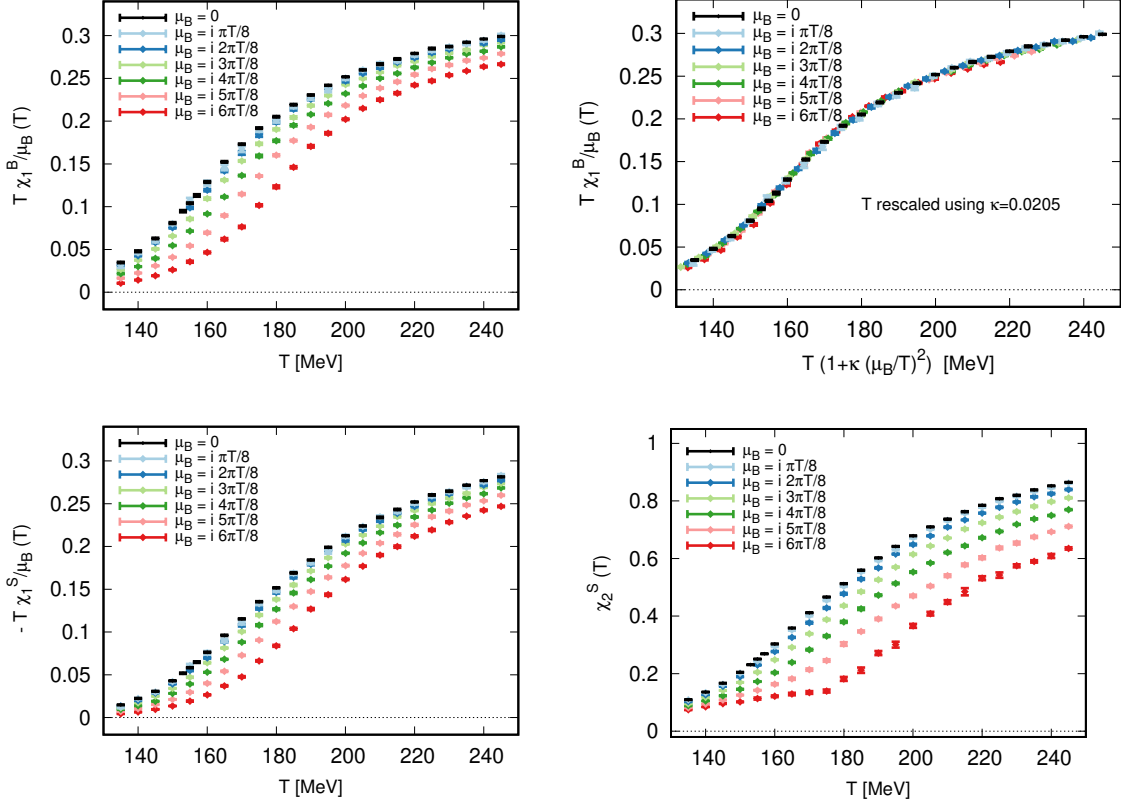


**Figure 1:** (Top left panel): Normalized baryon density at imaginary baryon chemical potentials. The points at  $\mu_B = 0$  (black) show the second baryon susceptibility  $\chi_2^B(T)$ . (Top right panel): Same as in the left panel, with the temperature rescaled in accordance to Eq. (1) with  $\kappa = 0.0205$ . (Bottom left panel): Normalized strangeness density at imaginary baryon chemical potentials. The points at  $\mu_B = 0$  (black) show the mixed baryon strangeness susceptibility  $\chi_{11}^{BS}(T)$ . (Bottom right panel): Second strangeness susceptibility  $\chi_2^S(T)$  at zero and imaginary baryon chemical.

## 2. The alternative expansion scheme

The starting point of our procedure is noticing that certain fluctuation observables display a similar structure at all the imaginary chemical potentials we simulate. This is the case for both the baryon and strangeness densities (normalized by  $\hat{\mu}_B$ ), as well as for the second strangeness susceptibility, as shown in Fig. 1. For the (normalized) baryon and strangeness densities, one can easily notice that the limit  $\hat{\mu}_B \rightarrow 0$  equals  $\chi_2^B$  and  $\chi_{11}^{BS}$ , respectively.

Let us take a look at the (normalized) baryon density first. As a consequence of the similarity of its temperature dependence at different chemical potential, its  $\hat{\mu}_B$  behavior can be captured through a  $\hat{\mu}_B$ -dependent rescaling of the temperature. In fact, a single temperature-independent parameter is able to describe such rescaling quite well:

$$\frac{\chi_1^B(T, \hat{\mu}_B)}{\hat{\mu}_B} = \chi_2^B(T', 0), \quad T' = (1 + \kappa \hat{\mu}_B^2). \quad (1)$$

<sup>1</sup>We use the following notation for the dimensionless chemical potentials:  $\hat{\mu}_i = \mu_i/T$ .

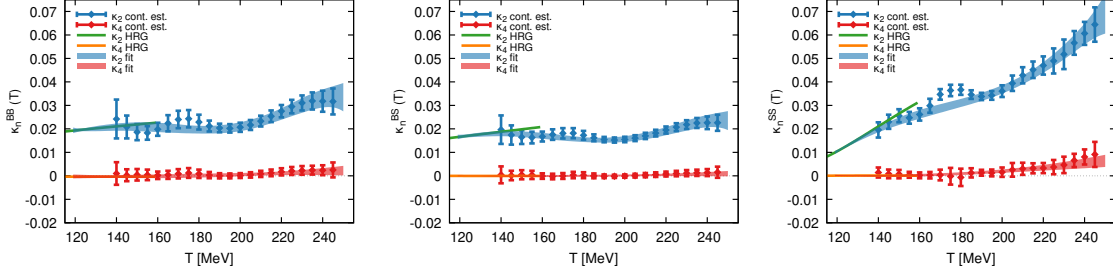


**Figure 2:** Continuum extrapolated result for the expansion parameters  $\kappa_2^{ij}(T)$  and  $\kappa_4^{ij}(T)$ . HRG results are shown up to  $T = 160$  MeV (in green for  $\kappa_2^{ij}$ , orange for  $\kappa_4^{ij}$ , respectively). The bands show correlated polynomial fits.

Such a simple rescaling of the temperature makes all the curves collapse onto each other, as shown in the top right panel of Fig. 1. Analogous observations can be made for both  $\chi_1^S$  and  $\chi_2^S$ , with:

$$\frac{\chi_1^S(T, \hat{\mu}_B)}{\hat{\mu}_B} = \chi_{11}^{BS}(T', 0), \quad \chi_2^S(T, \hat{\mu}_B) = \chi_2^S(T', 0). \quad (2)$$

The fact that a single parameter, not depending on the temperature, can describe the shift we observe in the observables of interest, suggests that the next-order parameter would probably be sensibly smaller in magnitude. In order to define our expansion scheme in a rigorous manner, we add higher order expansion parameters, and let them depend on the temperature:

$$T' = T \left( 1 + \kappa_2^{ij}(T) \hat{\mu}_B^2 + \kappa_4^{ij}(T) \hat{\mu}_B^4 + O(\hat{\mu}_B^6) \right), \quad (3)$$

where the  $k_n^{ij}(T)$  now indicate that they can refer to either one of the observables we consider.

We stress that the expansion scheme we propose is essentially a reorganization of the Taylor series. Rather than carrying out the expansion at  $T = \text{const}$  as in the Taylor method, we follow “lines of constant physics”, namely trajectories in the  $T - \hat{\mu}_B$  plane where e.g.,  $\chi_1^B(T, \hat{\mu}_B)/\hat{\mu}_B$  is constant. In fact, the rhs of e.g., Eq.(1) is effectively expanded in  $\Delta T = T' - T$ . Working out expansions of both the lhs and rhs, then equating equal order terms, one finds

$$\kappa_2^{BB}(T) = \frac{1}{6T} \frac{\chi_4^B(T)}{\chi_2^{B'}(T)}, \quad \kappa_4^{BB}(T) = \frac{1}{360 \chi_2^{B'}(T)^3} \left( 3 \chi_2^{B'}(T)^2 \chi_6^B(T) - 5 \chi_2^{B''}(T) \chi_4^B(T)^2 \right), \quad (4)$$

with analogous relations holding for the other observables.

### 3. Results

In order to calculate  $\kappa_n^{ij}(T)$ , we could simply take Eq.(4) at face value. However, large cancellations would likely appear in  $\kappa_4^{ij}(T)$ . Instead, we choose to exploit our simulations at imaginary chemical potentials  $\hat{\mu}_B = in\pi/8$ , with  $n = 0, \dots, 8$ . First, we construct the proxy quantity:

$$\Pi(T, \hat{\mu}_B^2) = \frac{T' - T}{T \hat{\mu}_B^2} = \kappa_2(T) + \kappa_4(T) \hat{\mu}_B^2 + O(\hat{\mu}_B^4), \quad (5)$$

at different temperatures and chemical potentials. At  $\hat{\mu}_B = 0$ , we simply have  $\Pi(T, 0) = \kappa_2^{ij}(T)$ . At finite  $\hat{\mu}_B$ ,  $T'$  is first determined by solving e.g., Eq. (1) for  $T'$ . For this, we first perform a spline fit to the data at zero and finite chemical potentials. Then, we can calculate  $\Pi(T, \hat{\mu}_B^2)$  for different chemical potentials, temperature-by-temperature. We include results from  $32^3 \times 8$ ,  $40^3 \times 10$ ,  $48^3 \times 12$  and  $64^3 \times 16$  lattices.

Finally, we perform a combined fit of  $\Pi(T, \hat{\mu}_B^2)$  in  $\hat{\mu}_B^2$  and  $1/N_\tau^2$ , from which we extract the continuum-extrapolated  $\kappa_2^{ij}$  and  $\kappa_4^{ij}$  at each temperature. In order to perform a systematic analysis of the errors, we carry out our procedures many times, then combine the results to include both statistical and systematic uncertainties. We include three different spline fits at  $\hat{\mu}_B = 0$ , and two at  $\hat{\mu}_B \neq 0$ . For the scale setting, we utilize either  $f_\pi$ , or  $w_0$  [22]. As ranges in the imaginary chemical potential included in the fit, we consider  $\text{Im } \hat{\mu}_B \leq 2.0$  or  $\text{Im } \hat{\mu}_B \leq 2.4$ . For the final fit, we consider fits that are linear in  $1/N_\tau^2$ , and linear, quadratic or 1/linear for the continuum limit. Finally, we either include or drop the  $N_\tau = 8$  results. Considering all possible combinations, this amounts to 144 separate analyses. After dropping those with a Q-values below 0.01, we weigh the results uniformly to obtain our final results. For a more detailed account of the treatment of the systematics, see Refs. [1, 14].

The different coefficients  $\kappa_n^{ij}(T)$  are shown in Fig. 2, together with the results of polynomial fits which take into account the full correlations between different temperatures. We show at low temperature results from the hadron resonance gas (HRG) model, in good agreement with our results. As expected, we find a large separation in the magnitudes of  $\kappa_2^{ij}(T)$  and  $\kappa_4^{ij}(T)$ , suggesting that convergence should be faster with this expansion.

To reconstruct thermodynamic quantities at real chemical potential, we simply employ Eq. (1) (similarly, for the strangeness density and second susceptibility, we employ Eq (2)), starting from  $\chi_2^B(T)$ . We then obtain the pressure by integrating over the chemical potential:

$$\frac{p(\mu_B, T)}{T^4} = \hat{p}(\hat{\mu}_B, T) = \hat{p}(0, T) + \int_0^{\hat{\mu}_B} d\hat{\mu}'_B \hat{n}_B(\hat{\mu}'_B, T), \quad (6)$$

and all other thermodynamic quantities follow.

Fig. 3 shows the baryon density (top left), pressure (top right), entropy density (center left), energy density (center right), strangeness density (bottom left) and strangeness second susceptibility (bottom right) in the range  $T = 130 - 240$  MeV, for  $\hat{\mu}_B \leq 3.5$ . We see that the uncertainties are under control in all cases, and good agreement with the HRG model is observed also at finite  $\hat{\mu}_B$ . Moreover, no unphysical, nonmonotonic behavior is present. For the baryon density, we additionally show (darker shades) the case in which  $\kappa_4^{BB} = 0$ . We notice that the effect of including this additional parameter is only that of increasing the error, while the value itself is barely affected. This further suggests that our series expansion possesses good convergence properties.

## Acknowledgments

This project was funded by the DFG grant SFB/TR55. The project also received support from the BMBF Grant No. 05P18PXFCA. This work was also supported by the Hungarian National Research, Development and Innovation Office, NKFIH grant KKP126769. A.P. is supported by the J. Bolyai Research Scholarship of the Hungarian Academy of Sciences and by the ÚNKP-20-5 New

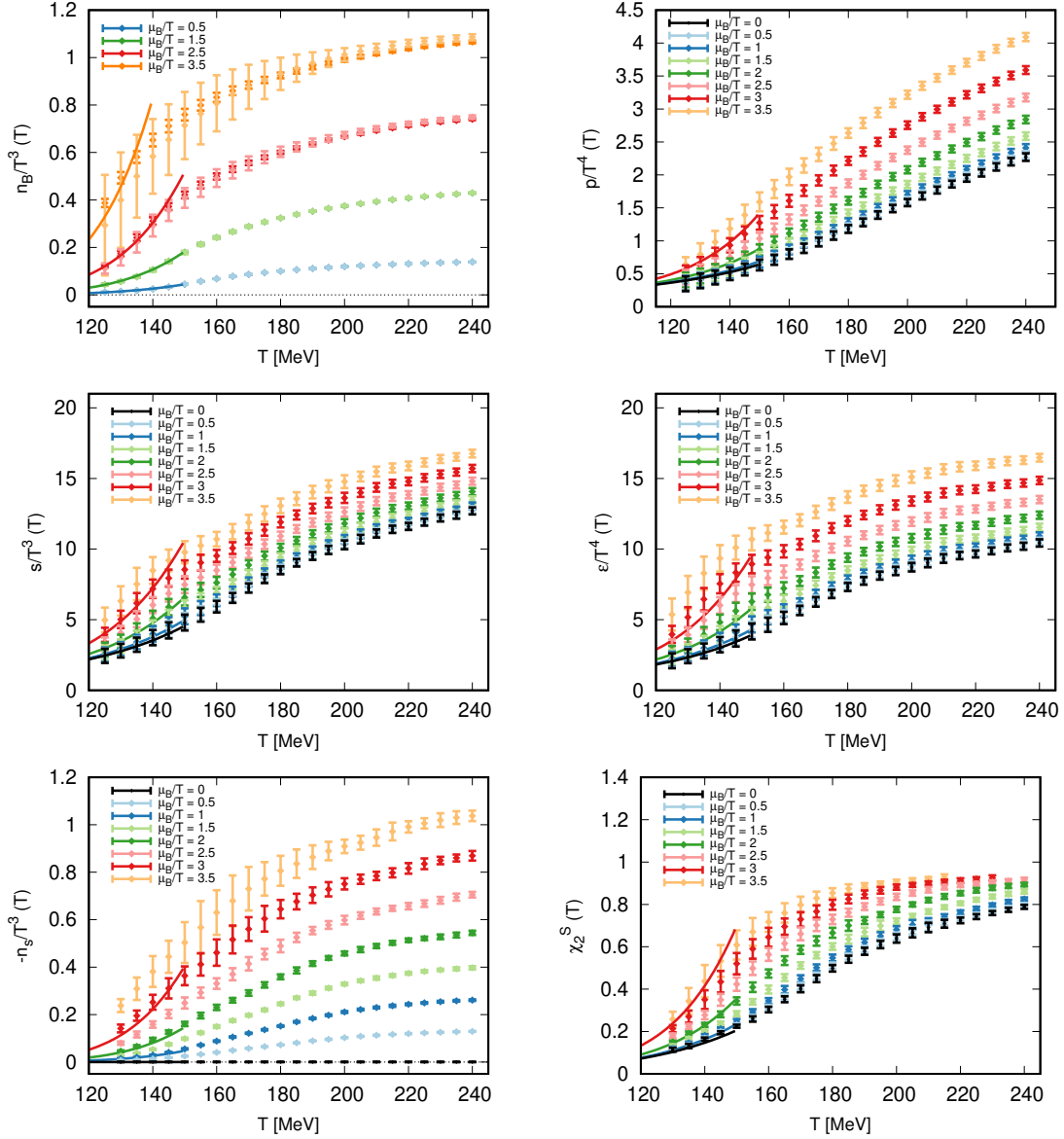


**Figure 3:** From top to bottom, left to right: baryon density, pressure, entropy density, energy density, strangeness density and strangeness second susceptibility. The results are shown at increasing values of  $\hat{\mu}_B$ . With solid lines we show the results from the HRG model. For the baryon density we also show in darker shades the results obtained by setting  $\kappa_4^{BB} \equiv 0$ .

National Excellence Program of the Ministry for Innovation and Technology. The project leading to this publication has received funding from Excellence Initiative of Aix-Marseille University - A\*MIDEX, a French “Investissements d’Avenir” programme, AMX-18-ACE-005. This material is based upon work supported by the National Science Foundation under grants no. PHY-1654219 and by the U.S. DoE, Office of Science, Office of Nuclear Physics, within the framework of the Beam Energy Scan Topical (BEST) Collaboration. This research used resources of the Oak Ridge Leadership Computing Facility, which is a DOE Office of Science User Facility supported

under Contract DE-AC05-00OR22725. The authors gratefully acknowledge the Gauss Centre for Supercomputing e.V. ([www.gauss-centre.eu](http://www.gauss-centre.eu)) for funding this project by providing computing time on the GCS Supercomputer HAWK at HLRS, Stuttgart. Part of the computation was performed on the QPACE3 funded by the DFG and hosted by JSC. C.R. also acknowledges the support from the Center of Advanced Computing and Data Systems at the University of Houston.

## References

- [1] S. Borsányi, Z. Fodor, J. N. Guenther, R. Kara, S. D. Katz, P. Parotto, A. Pásztor, C. Ratti and K. K. Szabó, *Phys. Rev. Lett.* **126**, no.23, 232001 (2021) doi:10.1103/PhysRevLett.126.232001 [arXiv:2102.06660 [hep-lat]].
- [2] Y. Aoki, G. Endrodi, Z. Fodor, S. D. Katz and K. K. Szabo, *Nature* **443**, 675-678 (2006) doi:10.1038/nature05120 [arXiv:hep-lat/0611014 [hep-lat]].
- [3] S. Borsanyi, G. Endrodi, Z. Fodor, A. Jakovac, S. D. Katz, S. Krieg, C. Ratti and K. K. Szabo, *JHEP* **11**, 077 (2010) doi:10.1007/JHEP11(2010)077 [arXiv:1007.2580 [hep-lat]].
- [4] S. Borsanyi, Z. Fodor, C. Hoelbling, S. D. Katz, S. Krieg and K. K. Szabo, *Phys. Lett. B* **730**, 99-104 (2014) doi:10.1016/j.physletb.2014.01.007 [arXiv:1309.5258 [hep-lat]].
- [5] A. Bazavov *et al.* [HotQCD], *Phys. Rev. D* **90**, 094503 (2014) doi:10.1103/PhysRevD.90.094503 [arXiv:1407.6387 [hep-lat]].
- [6] D. Sexty, *Phys. Rev. D* **100**, no.7, 074503 (2019) doi:10.1103/PhysRevD.100.074503 [arXiv:1907.08712 [hep-lat]].
- [7] M. Giordano, K. Kapas, S. D. Katz, D. Nogradi and A. Pásztor, *Phys. Rev. D* **102**, no.3, 034503 (2020) doi:10.1103/PhysRevD.102.034503 [arXiv:2003.04355 [hep-lat]].
- [8] M. Giordano, K. Kapas, S. D. Katz, D. Nogradi and A. Pásztor, *JHEP* **05**, 088 (2020) doi:10.1007/JHEP05(2020)088 [arXiv:2004.10800 [hep-lat]].
- [9] S. Borsanyi, Z. Fodor, M. Giordano, S. D. Katz, D. Nogradi, A. Pásztor and C. H. Wong, [arXiv:2108.09213 [hep-lat]].
- [10] C. R. Allton, S. Ejiri, S. J. Hands, O. Kaczmarek, F. Karsch, E. Laermann, C. Schmidt and L. Scorzato, *Phys. Rev. D* **66**, 074507 (2002) doi:10.1103/PhysRevD.66.074507 [arXiv:hep-lat/0204010 [hep-lat]].
- [11] S. Borsanyi, G. Endrodi, Z. Fodor, S. D. Katz, S. Krieg, C. Ratti and K. K. Szabo, *JHEP* **08**, 053 (2012) doi:10.1007/JHEP08(2012)053 [arXiv:1204.6710 [hep-lat]].
- [12] P. de Forcrand and O. Philipsen, *Nucl. Phys. B* **642**, 290-306 (2002) doi:10.1016/S0550-3213(02)00626-0 [arXiv:hep-lat/0205016 [hep-lat]].
- [13] M. D'Elia and M. P. Lombardo, *Phys. Rev. D* **67**, 014505 (2003) doi:10.1103/PhysRevD.67.014505 [arXiv:hep-lat/0209146 [hep-lat]].

- [14] S. Borsanyi, Z. Fodor, J. N. Guenther, S. K. Katz, K. K. Szabo, A. Pasztor, I. Portillo and C. Ratti, *JHEP* **10**, 205 (2018) doi:10.1007/JHEP10(2018)205 [arXiv:1805.04445 [hep-lat]].
- [15] A. Bazavov, D. Bollweg, H. T. Ding, P. Enns, J. Goswami, P. Hegde, O. Kaczmarek, F. Karsch, R. Larsen and S. Mukherjee, *et al.* *Phys. Rev. D* **101**, no.7, 074502 (2020) doi:10.1103/PhysRevD.101.074502 [arXiv:2001.08530 [hep-lat]].
- [16] A. Bazavov *et al.* [HotQCD], *Phys. Lett. B* **795**, 15-21 (2019) doi:10.1016/j.physletb.2019.05.013 [arXiv:1812.08235 [hep-lat]].
- [17] S. Borsanyi, Z. Fodor, J. N. Guenther, R. Kara, S. D. Katz, P. Parotto, A. Pasztor, C. Ratti and K. K. Szabo, *Phys. Rev. Lett.* **125**, no.5, 052001 (2020) doi:10.1103/PhysRevLett.125.052001 [arXiv:2002.02821 [hep-lat]].
- [18] R. Bellwied, S. Borsanyi, Z. Fodor, S. D. Katz, A. Pasztor, C. Ratti and K. K. Szabo, *Phys. Rev. D* **92**, no.11, 114505 (2015) doi:10.1103/PhysRevD.92.114505 [arXiv:1507.04627 [hep-lat]].
- [19] N. Haque and M. Strickland, *Phys. Rev. C* **103**, no.3, 031901 (2021) doi:10.1103/PhysRevC.103.L031901 [arXiv:2011.06938 [hep-ph]].
- [20] N. Dupuis, L. Canet, A. Eichhorn, W. Metzner, J. M. Pawłowski, M. Tissier and N. Wschebor, *Phys. Rept.* **910**, 1-114 (2021) doi:10.1016/j.physrep.2021.01.001 [arXiv:2006.04853 [cond-mat.stat-mech]].
- [21] V. Dexheimer, J. Noronha, J. Noronha-Hostler, C. Ratti and N. Yunes, *J. Phys. G* **48**, no.7, 073001 (2021) doi:10.1088/1361-6471/abe104 [arXiv:2010.08834 [nucl-th]].
- [22] S. Borsanyi, S. Durr, Z. Fodor, C. Hoelbling, S. D. Katz, S. Krieg, T. Kurth, L. Lelouch, T. Lippert and C. McNeile, *et al.* *JHEP* **09**, 010 (2012) doi:10.1007/JHEP09(2012)010 [arXiv:1203.4469 [hep-lat]].